Gallocatechin biosynthesis via a flavonoid 3',5'-hydroxylase is a defense response in Norway spruce against infection by the bark beetle-associated sap-staining fungus *Endoconidiophora polonica*

Almuth Hammerbacher[1, 2, *], Bettina Raguschke[2], Louwrance P. Wright[2,3] and Jonathan Gershenzon[2]

[1] Department of Zoology and Entomology, Forestry and Agricultural Biotechnology Institute, University of Pretoria, Private Bag X20, Pretoria 0028, South Africa; almuth.hammerbacher@fabi.up.ac.za

[2] Department of Biochemistry, Max Planck Institute for Chemical Ecology, Hans-Knoell Str. 8, 07745 Jena, Germany; raguschke@ice.mpg.de (BR); gershenzon@ice.mpg.de (JG)

[3] Zeiselhof Research Farm, P.O. Box 35984, Menlo Park 0102, Pretoria, South Africa; lwright@tutanota.com

[*] Correspondence: almuth.hammerbacher@fabi.up.ac.za; Tel: +27 12 420 3934;
Fax: +27 12 420 3960

Highlights

- Norway spruce produces 2,3-*trans*-gallocatechin in response to fungal infection.
- Flavonoid 3′,5′-hydroxylase catalyzes the conversion of catechin to gallocatechin.
- Gallocatechin inhibits melanin accumulation in a bark beetle associated fungus.

Graphical abstract: Gallocatechin biosynthesis via a flavonoid 3',5'-hydroxylase is a defense response in Norway spruce bark and wood against infection by the bark beetle-associated sap-staining fungus *Endoconidiophora polonica*.

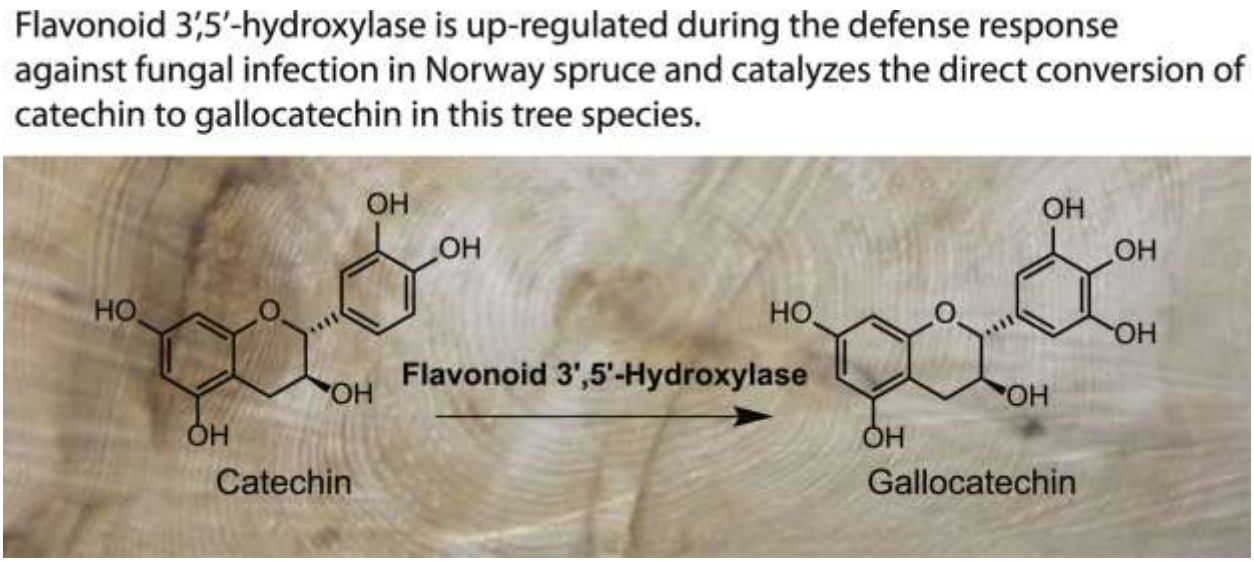

Abstract:

One of the best-studied defense responses to fungal infection in Norway spruce (*Picea abies*) is the biosynthesis of flavan-3-ols, which accumulate as monomers or polymers known as proanthocyanidins. The individual flavan-3-ol units consist of compounds with a 3',4'-dihydroxylated B ring [2,3-(*trans*)-(+)-catechin or 2,3-(*cis*)-(-)-epicatechin] and compounds with a 3',4',5'-trihydroxylated B ring [2,3 (*trans*)-(+)-gallocatechin or 2,3-(*cis*)-(-)-epigallocatechin]. While much is known about the biosynthesis and biological activity of catechin in Norway spruce, there is little comparable information about gallocatechin or epigallocatechin. We found that there was a significant increase in the gallocatechin content of Norway spruce bark and wood after inoculation with the bark beetle-associated sap-staining fungus *Endoconidiophora polonica.* Gallocatechins increased proportionally more than catechins as both monomers and units of polymers. A flavonoid 3',5'-hydroxylase gene identified in Norway spruce was shown by heterologous expression in *Nicotiana benthamiana* to be involved in the conversion of 2,3 (*trans*)-(+)-catechin to 2,3 (*trans*)-(+)-gallocatechin. The formation of the trihydroxylated B ring in Norway spruce occurs at the level of flavan-3-ols, rather than at the level of dihydroflavonols as in many angiosperms. The transcript abundance of the flavonoid 3',5'-hydroxylase gene also increased significantly during fungal infection underlining its importance in gallocatechin

biosynthesis. Comparisons of the effect of 2,3 (*trans*)-(+)-catechin and 2,3 (*trans*)-(+)-gallocatechin on fungal growth revealed that 2,3 (*trans*)-(+)-catechin is a stronger inhibitor of fungal growth, while 2,3 (*trans*)-(+)-gallocatechin is a stronger inhibitor of melanin biosynthesis.

Keywords: gallocatechin, flavonoid 3',5'-hydroxylase, Norway spruce, *Picea abies*, *Endoconidiophora polonica*, blue-stain fungus, anti-fungal defense

1. Introduction

Norway spruce (*Picea abies* Karst. L) is a conifer endemic to Europe and Northern Asia. Growing mainly in mountainous and boreal regions, this tree species is ecologically and economically important due to its fast growth, dominance in the landscape and its ability to fix large amounts of carbon dioxide (Nystedt et al., 2013). Under dry and hot conditions Norway spruce becomes susceptible to mass attack by the European bark beetle *Ips typographus* (Stadelmann et al., 2013). Successful attack by this beetle can cause huge losses of mature spruce trees encompassing large areas (Schlyter et al., 2006).

The European bark beetle is associated with numerous sap-staining fungi that infect trees while the beetles bore into the inner bark to lay their eggs (Krokene and Solheim, 1998). The best-studied fungal associate of *I. typographus*, *Endoconidiophora polonica*, has been shown to kill healthy trees without the intervention of the bark beetle (Krokene, 2015). During infection the fungus elicits the biosynthesis of terpenoid oleoresin and phenolic compounds in Norway spruce (Franceschi et al., 2005). By over-stimulating defense responses, the fungus is thought to exhaust the tree's energy and thus contributes to successful bark beetle establishment in the phloem (Paine et al., 1997). *Endoconidiophora polonica* itself can successfully circumvent the toxic effects of some host defenses by degrading them and using them as a carbon source (Hammerbacher et al., 2013).

Among the best studied defense responses to fungal infection in Norway spruce is the biosynthesis of proanthocyanidins (PAs; condensed tannins; Hammerbacher et al., 2014; Nemesio-Gorritz et al., 2016). These polymeric compounds are composed of flavan-3-ol units with a basic C_6-C_3-C_6 flavonoid skeleton having an A-, B- and C-ring (Figure 1A). Depending on the stereochemistry of the asymmetric carbons on the C -ring, flavan-3-ols either occur in a 2,3-(*trans*)-(+)- or a 2,3-(*cis*)-(-)-configuration. PAs are formed by linkage of the C4 position of

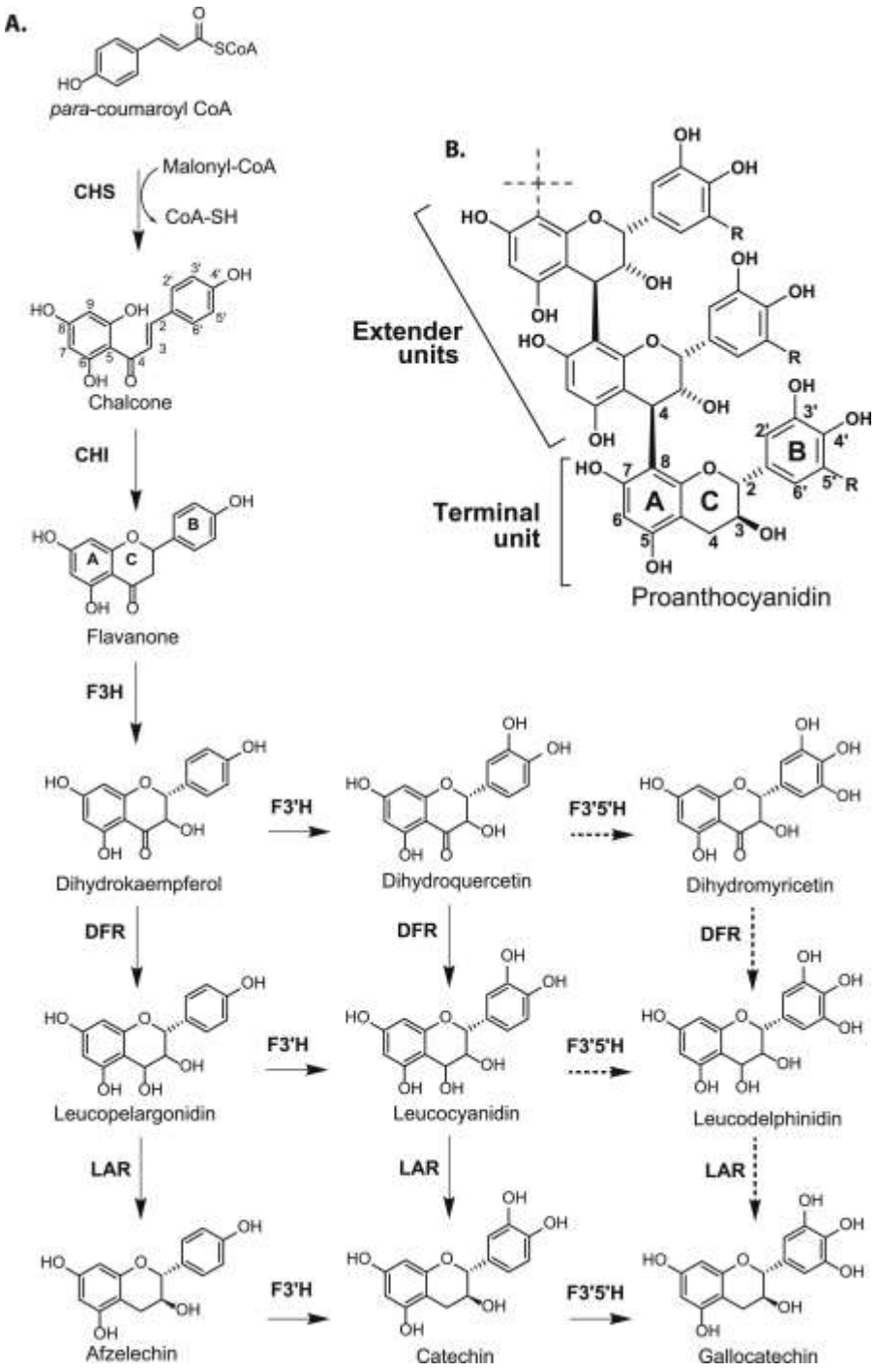

Figure 1: (A) Biosynthesis of monomeric flavan-3-ols via the flavonoid pathway. In Norway spruce, the pathway to gallocatechin leads through catechin rather than dihydromyricetin or leucodelphinidin. The third hydroxyl group of the B ring occurs at the level of the flavan-3-ols rather than at the level of dihydroflavonols as in angiosperms. Abbreviations: CoA, coenzyme A; CHS, chalcone synthase; CHI, chalcone isomerase; F3H, flavanone-3-hydroxylase; F3'H, flavonoid 3' hydroxylase; F3'5'H, flavonoid 3'5'-hydroxylase; DFR, dihydroflavonol reductase; LAR, leucoanthocyanidin reductase. (B) Structure of a proanthocyanidin, a polymer of flavan-3-ol units, joined by C_4-C_8 bonds.

extender units to the C8 position of the terminal unit and the entire polymer can be many units long (Figure 1B). The B-ring of flavan-3-ols can be either hydroxylated only on the 4'-position, giving rise to *cis* or *trans* (epi)afzelechin and ultimately propelargonidin PA polymers; they can be hydroxylated on the 3' and 4' positions, giving rise to *cis* or *trans* (epi)catechin and ultimately procyanidin PAs; or they can be hydroxylated at the 3', 4' and 5' positions yielding *cis* or *trans* (epi)gallocatechin and ultimately prodelphinidin PA polymers (Dixon et al., 2005).

Flavan-3-ols and PAs are the end-products of the flavonoid biosynthesis pathway. 2,3-(*trans*)-(+)-Flavan-3-ols are produced from leucocyanidin substrates via a reduction reaction carried out by leucoanthocyanidin reductases (LAR; Figure 1A; Tanner et al., 2003). 2,3-(*cis*)-(-)-Flavan-3-ols, on the other hand are synthesized from anthocyanidins by the enzymes anthocyanidin reductase (ANR; Xie et al., 2004). The number of hydroxyl groups on the B-ring is determined by the presence and activity of flavonoid 3'-hydroxylases (F3'H) catalyzing hydroxylation of the 3' position (Figure 1A) and flavonoid 3',5'-hydroxylases (F3'5'H) catalyzing hydroxylation of the 3' and 5' positions (Figure 1A; Tanaka and Brugliera, 2013). These enzymes are thought to predominantly hydroxylate dihydroflavanol substrates (Ishiguro et al., 2012), which are upstream intermediates in the flavonoid biosynthesis pathway two steps prior to flavan-3-ols. The mechanism by which PA polymers are synthesized is not fully understood, but from analysis of mutations in *Medicago truncatula* and *Arabidopsis thaliana* it is now believed that both ANR (Xie et al., 2004) and LAR (Liu et al., 2016) play important roles in the polymerization reaction and determine the length of the PA chain.

The major monomeric flavan-3-ol in Norway spruce under natural growth conditions is 2,3-(*trans*)-(+)-catechin, while the major component of PA polymers is 2,3-(*cis*)-(-)-epicatechin (Hammerbacher et al., 2014). During infection by the sap-staining fungus *E. polonica*, this profile changes with a larger percentage of monomeric 2,3-(*trans*)-(+)-gallocatechin as well as a larger percentage of 2,3-(*cis*)-(-)-epigallocatechin as a component of PA polymers (Hammerbacher et al., 2014). *Endoconidiophora polonica* is known to degrade flavan-3-ols with dihydroxylated aromatic rings, such as catechin and epicatechin, via the beta-ketoadipate pathway to CO_2 (Wadke et al., 2016). On the other hand, trihydroxylated B ring flavan-3-ols, such as gallocatechin and epigallocatechin, are not accepted as substrates by fungal catechol dioxygenase enzymes, which catalyze the first step in this catabolic pathway (Wadke et al., 2016). Therefore, a change in flavan-3-ol composition from compounds with dihydroxylated B

rings to those with trihydroxylated B rings may create products that cannot be utilized by the fungus. However, it is not known how 2,3-(*trans*)-(+)- or 2,3-(*cis*)-(-)-(epi)gallocatechin is synthesized in this tree species, nor is it known if these compounds are effective defenses against fungi infecting Norway spruce.

In order to address these questions, we infected Norway spruce saplings with *E. polonica.* Fungal infection changed the flavan-3-ol profile from dihydroxylated to trihydroxylated B ring compounds in bark and wood. A F3'5'H gene was identified in Norway spruce, which was functionally characterized by overexpressing the whole flavan-3-ol biosynthesis pathway in *Nicotiana benthamiana* and profiling transcript levels of this gene in infected spruce bark and wood. We also compared the biological activities of 2,3-(*trans*)-(+)-catechin and 2,3-(*trans*)-(+)-gallocatechin by conducting *in vitro* growth assays with *E. polonica*.

2. Results and Discussion

2.1. Gallocatechin, catechin and their proanthocyanidin polymers accumulate in Norway spruce upon infection with E. polonica

Norway spruce saplings were wounded or wounded and inoculated with the sap-staining fungus *E. polonica,* and the catechin content in bark and wood were analyzed by LC-MS over a time course of 28 d. Concentrations of 2,3-(*trans*)-(+)-catechin and 2,3-(*trans*)-(+)-gallocatechin increased significantly over the infection period in inoculated bark and wood compared to the wounded control treatments with gallocatechin showing a much greater proportional increase (Figure 2). In bark, a significant increase in 2,3-(*trans*)-(+)-catechin was recorded at 14 and 28 days post inoculation (dpi) after fungal inoculation ($p < 0.001$; Figure 2 A), whereas there was no significant increase over the whole experimental period in wounded controls. Fungal lesions at 14 and 28 d post-infection were separated into two sections: fungus that was already established at the onset of the experiment (inner lesion) and newly infected tissue (outer lesion). Interestingly, both outer and inner lesion sections contained higher levels of 2,3-(*trans*)-(+)-catechin ($p < 0.05$) than the wounded control, showing that catechin biosynthesis in response to fungal infection occurs at a faster rate than fungal degradation of this compound reported previously (Wadke et al., 2016).

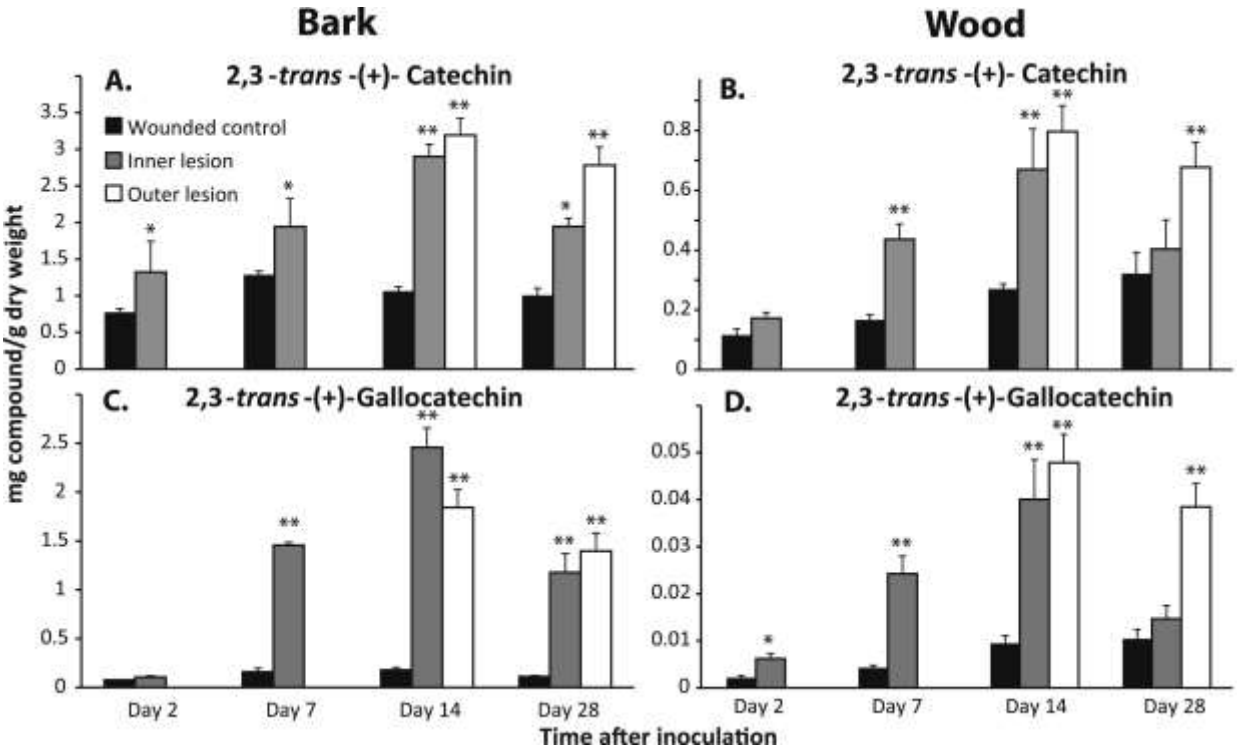

Figure 2: Accumulation of flavan-3-ol monomers in the bark (A and C) and wood (B and D) of Norway spruce saplings after infection by *E. polonica* compared to saplings that were wounded without infection. Both 2,3-*trans*-catechin (upper panels) and 2,3-*trans*-gallocatechin (lower panels), as measured by LC-tandem mass spectrometry, increased significantly at 14 and 28 days after infection ($p < 0.01$) in the lesions of inoculated trees ($n = 5$; error bars = SE; stars denote treatments significantly different from the control).

In wood 2,3-(*trans*)-(+)-catechin levels increased significantly at 7 d after infection ($p < 0.01$), earlier than in bark, reaching a maximum at 14 d followed by a decrease at 28 d (Figure 2B). This decrease was most evident in the inner lesion. 2,3-(*trans*)-(+)-Catechin in the wounded controls in wood also increased steadily over the 28 d period, unlike in bark, with significantly more compound at 28 d than at 2 dpi ($p < 0.05$).

Similar increases in 2,3-(*trans*)-(+)-catechin in Norway spruce bark and wood were previously observed in response to *E. polonica* infection (Hammerbacher et al., 2014) in saplings as well as in mature stems infected with the spruce root rot fungus *Heterobasidion annosum* (Danielsson et al., 2011). The biosynthesis of 2,3-(*trans*)-(+)-catechin therefore seems to be closely connected to other defense responses to fungal invasion in Norway spruce. However, the success of this defense response might be variable, depending on the ability of the invading fungal species to circumvent it by detoxification, utilization as a nutrient source or another counter adaptation (Wadke et al., 2016).

Levels of the catechin with the trihydroxylated B-ring, 2,3-(*trans*)-(+)-gallocatechin, increased significantly after fungal inoculation in both bark and wood at 7 dpi ($p < 0.001$), reached a maximum at 14 dpi and then decreased at 28 dpi (Figure 2 C and D). This decrease was significant in the inner lesions of both bark and wood ($p < 0.05$) and might be explained by degradation of this compound by *E. polonica* or incorporation of this metabolite into proanthocyanidin (PA) polymers (Figure 3).

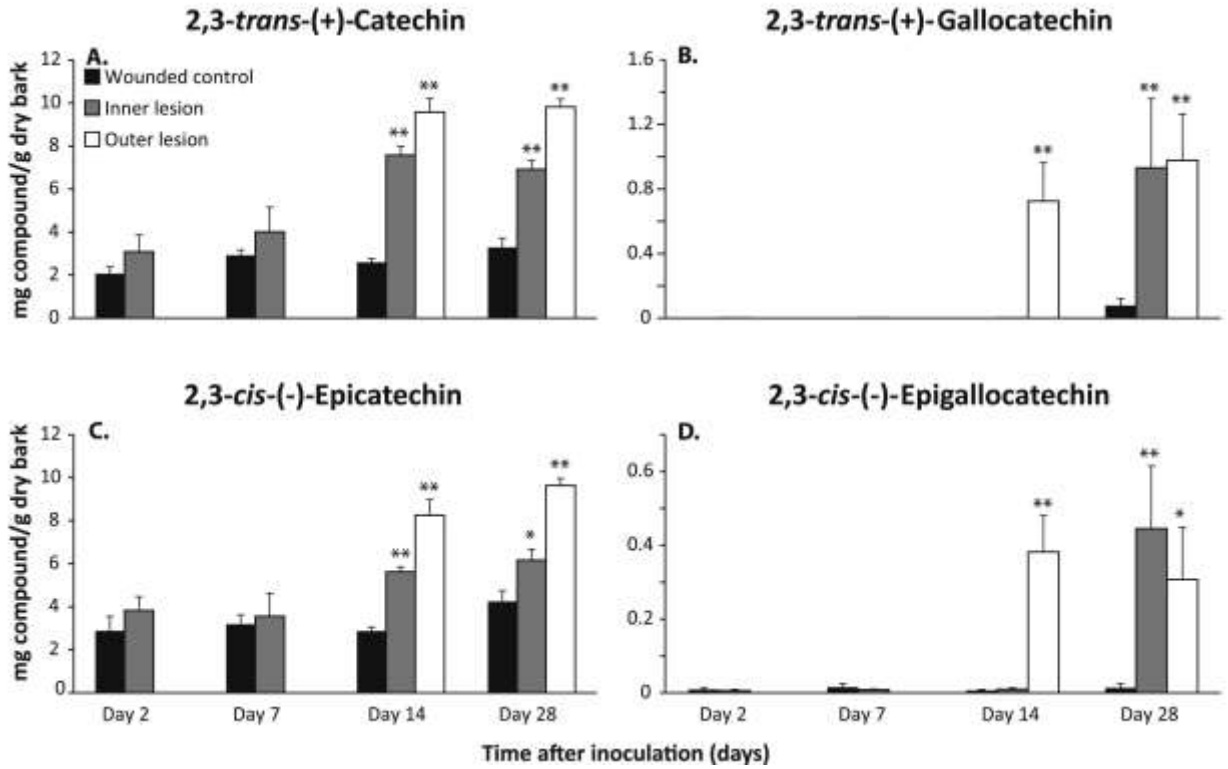

Figure 3: Accumulation of flavan-3-ol units in PA polymers in the bark of Norway spruce saplings after infection by *E. polonica*. Flavan-3-ol units with both dihydroxylated (left panels) and trihydroxylated (right panels) B-rings significantly increased at 14 and 28 days after infection in the outer lesions ($p < 0.01$) and at 28 days in the inner lesions of inoculated trees compared to saplings wounded without fungal infection ($n = 5$; error bars = SE; stars denote treatments significantly different from the control). Acid hydrolysis of PAs was achieved with trifluroacetic acid at 65℃ in the presence of sodium cyanoborohydride as a reducing agent. Hydrolysis products were analyzed using LC-tandem mass spectrometry.

Accumulation of flavan-3-ols in PA polymers was quantified in the bark of Norway spruce saplings by hydrolyzing the PAs with trifluroacetic acid in the presence of sodium cyanoborohydride as a reducing agent (Hammerbacher et al., 2013). Levels of 2,3-(*trans*)-(+)-catechin in the hydrolysate followed the same trends observed for the free monomers with

increased amounts at 14 and 28 d after infection (Figure 3 A; $p < 0.001$). The hydrolysate also contained the monomer 2,3-(*cis*)-(-)-epicatechin which also increased during the later stages of fungal infection ($p < 0.001$; Figure 3 B). 2,3-(*trans*)-(+)-Gallocatechin (Figure 3 C) and 2,3-(*cis*)-(-)-epigallocatechin (Figure 3 D) were present in the PA's of infected saplings at very low concentrations or were entirely absent from 2 to 7 dpi. However, at 14 d post-inoculation both 2,3-(*trans*)-(+)-gallocatechin and 2,3-(*cis*)-(-)-epigallocatechin were detected in PAs extracted from the region where the fungus had just started to colonize the tissue (outer lesion) and at 28 dpi both compounds were detected in the inner as well as the outer lesion and low amounts were even detected in the wounded control.

The percentage of 2,3-(*trans*)-(+)-gallocatechin in the monomeric flavan-3-ol fraction in bark increased from 25% at 2 dpi to 40% at 14 dpi in the inner lesion. A similar trend was observed in wood with an increase from 2% 2,3-(*trans*)-(+)-gallocatechin in the monomeric flavan-3-ol mixture at 2 dpi compared to 7% at 14 dpi in the inner lesion. In PA polymers an increase in the total percentage of flavan-3-ols with a trihydroxylated B-ring from less than 1% at 2 dpi to 5 – 6% in the outer lesion at 28 dpi was observed. This increase in the gallocatechin:catechin ratio during infection by *E. polonica* can be explained by either of two possible scenarios: (1) preferential biosynthesis of 2,3-(*trans*)-(+)-gallocatechin elicited by fungal infection (Hammerbacher et al., 2014) or (2) preferential catabolism of catechin by the fungus resulting in higher levels of gallocatechin in the infected tissues (Wadke et al., 2016). Either way, the increased amounts of 2,3-(*trans*)-(+)-gallocatechin in the total flavan-3-ol mixture could contribute to increased tree resistance to fungal colonization.

2.2. Flavonoid 3' 5'-hydroxylase is encoded in Norway spruce by a single functional gene that is highly expressed during fungal infection

An annotation of the white spruce genome by Warren et al. (2015) revealed the presence of two *F3'5'H* genes in this species (CYP75A42 v.2 and CYP75A63). *F3'5'H* are expected to encode the cytochrome P450 monooxygenases adding the third B-ring hydroxyl group to gallocatechin and other flavonoids. However, BLAST searches using the predicted open reading frames of both putative genes in EST libraries from white spruce as well as Norway spruce (www.congenie.org; www.ncbi.nlm.nih.gov) yielded only contigs from a single mRNA transcript with high similarity to CYP75A42 v.2 (Warren et al., 2015). Similarly primers

designed to amplify the predicted open reading frames of the two genes from cDNA generated from different white and Norway spruce RNA samples yielded only the CYP75A42 product. The predicted CYP75A63 gene therefore does not appear to be transcribed in the Norway and white spruce genotypes used in our experiments under normal physiological conditions or during pathogen attack.

To measure gene expression, RNA was extracted from wounded and fungus-inoculated Norway spruce bark and wood using the same material as for the metabolite profiling. After transcription to cDNA, quantitative real-time PCR was carried out using primers designed to amplify a 200 bp fragment of the CYP75A42 v.2 transcript. Transcript abundance of CYP75A42 v.2 increased 4-fold in fungus-inoculated bark compared to that in the wounded control at 7 dpi and reached a maximum level of 10-fold at 14 dpi in the inner lesion (Figure 4 A; $p < 0.001$). In wood a similar pattern was observed, except that the maximum transcript abundance was reached at 7 dpi (Figure 4 B; $p < 0.001$). At 28 dpi transcript abundances of CYP75A42 v.2 returned to levels observed at 2 dpi and in the wounded control. Transcript levels in the outer lesion were lower or similar to those observed in the inner lesion. The relative transcript abundance of CYP75A42 v.2 thus correlated with the accumulation of 2,3-(*trans*)-(+)-gallocatechin in wood and bark (Figure 2 C and D) and is consistent with this gene encoding a functional F3’5’H enzyme.

A phylogenetic analysis of CYP75A42 v. 2 from Norway spruce, white spruce and loblolly pine in combination with other known F3’5’H and F3’H (CYP75B) protein sequences from flowering plants revealed that the CYP75A genes from conifers are significantly different from those of angiosperms. CYP75A42 v.2 was almost 98% similar in Norway spruce and white spruce. Spruce and pine CYP75A42 v.2 were 94% similar, but shared only 60 – 76% similarity with known F3’5’H proteins from angiosperms (Figure 5). Similar differences were found between gymnosperm and angiosperm F3’H sequences. Inclusion of gymnosperm sequences in our phylogenetic analysis indicated that F3’5’H and F3’H diverged before the appearance of angiosperms (Tanaka and Brugliera, 2013; Seitz et al., 2015) and that conifer *F3’5’H* genes are ancestral to those of flowering plants.

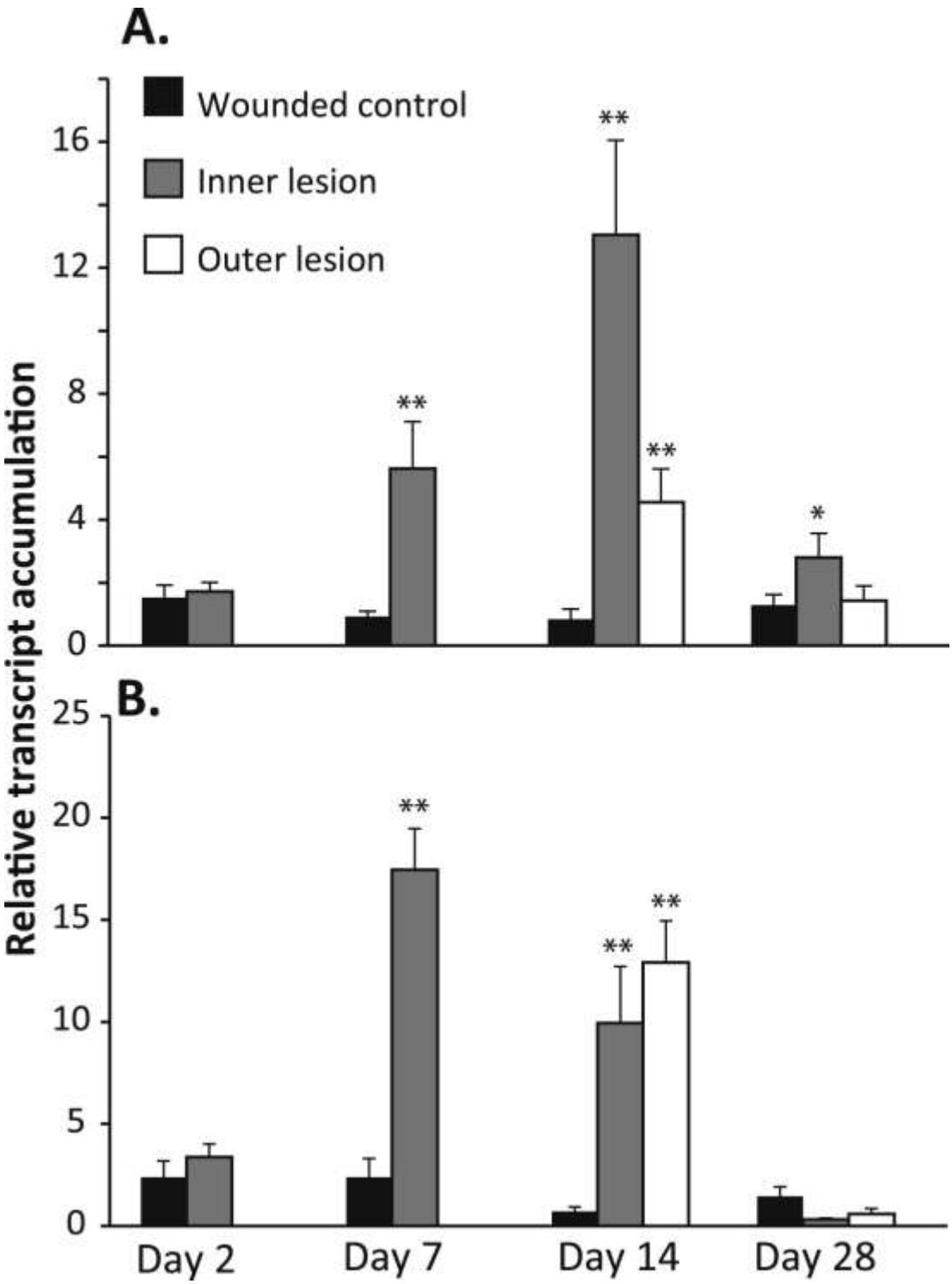

Figure 4: Transcript levels of *PaF3'5'H* increased after infection with *E. polonica* supporting its function in the production of gallocatechin. Transcript abundance of bark (A) and wood (B) was measured by qRT-PCR, normalized against *PaUBI* and calibrated against one replicate of the wounded control. Transcript abundance in the inner lesion differed significantly from that of the wounded only control ($p = 0.003$; n=5; error bars = SE; stars denote treatments significantly different from the control).

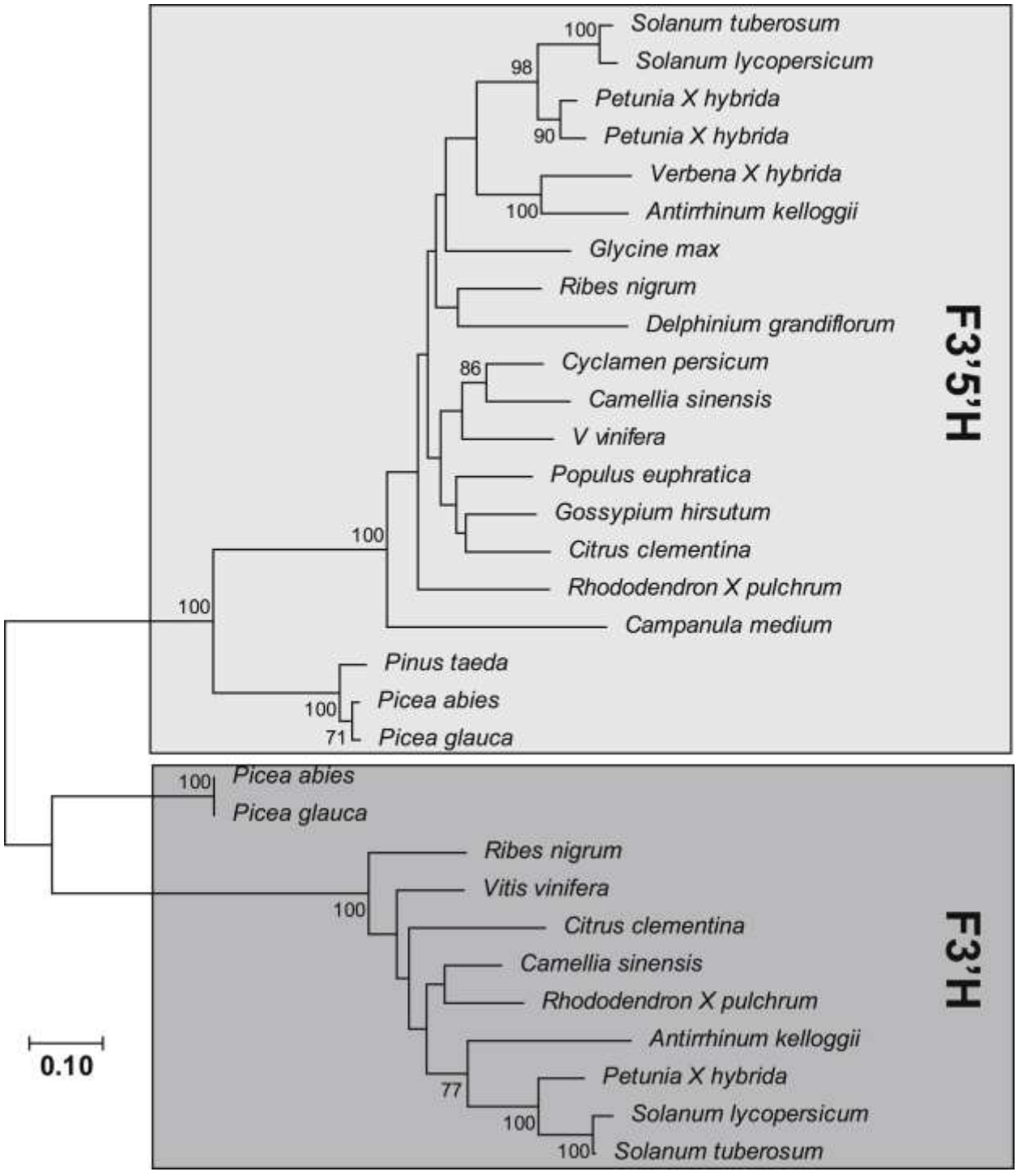

Figure 5: Evolution of F3'H and F3', 5'H enzymes. A maximum likelihood phylogenetic analysis of F3'H and F3',5'H enzyme classes from gymnosperms and angiosperms reveals separate lineages for genes encoding each enzyme type and, within each type, a separate clustering of gymnosperm and angiosperm sequences.

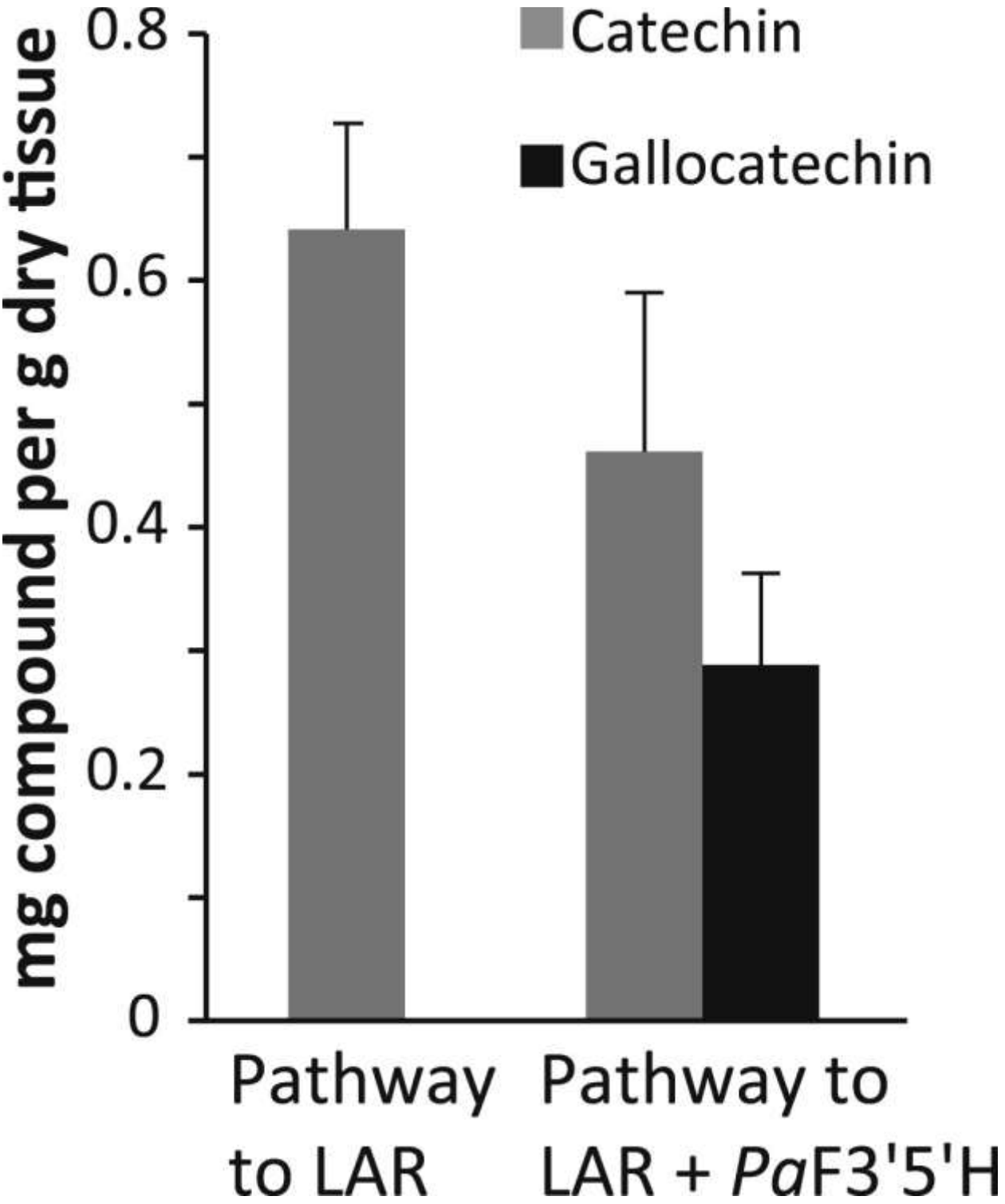

Figure 6: Norway spruce F3',5'H (Pa3',5'H) is involved in gallocatechin biosynthesis. *Nicotiana benthamiana* heterologously expressing all of the enzymes of the flavan-3-ol biosynthetic pathway up to leucoanthocyanidin reductase (LAR) produced catechin. Co-transformation with the gene encoding Pa3',5'H resulted in gallocatechin production. ($p = 0.003$; $n = 5$; error bars = SE)

2.3 Flavonoid 3'5'-hydroxylase is involved in gallocatechin biosynthesis in Norway spruce

In order to study the function of CYP75A42 v.2 from Norway spruce, the encoding gene was co-expressed with Norway spruce and apple genes encoding the rest of the flavonoid pathway, *PaCHS, PaF3H, PaF3'H, MdDFR* and *PaLAR3* (Figure 1), in *Nicotiana benthamiana* leaves using the transient expression protocols from Sainsbury et al. (2012). Since catechin accumulated in *N. benthamiana* leaves 7d after *Agrobacterium* infiltration, all genes must have been expressed and produced functional enzymes. Co-expression of these genes with CYP75A42 v.2 resulted in an accumulation additionally of 2,3-(*trans*)-(+)-gallocatechin in the leaves (Figure 6), indicating that the encoded F3'5'H enzyme is likely involved in gallocatechin formation in Norway spruce.

Current knowledge on the function of angiosperm F3'5'H indicates that the preferred substrates for this enzyme are dihydroflavonols (Figure 1). For example, in *Petunia* (Holton et al., 1993), *Antirrhinum kelloggii* (Ishiguro et al., 2012) as well as in the Asteraceae (Seitz et al., 2015) dihydroquercetin is preferentially hydroxylated by F3'5'H on the 5' position to produce dihydromyricetin before further metabolism to produce delphinidin, resulting in blue or purple flower color. In plants such as tea (Punjasiri et al., 2004) and grapevine (Castellarin et al., 2006), that accumulate high levels of flavan-3-ols, it was also shown that 5' hydroxylation preferentially occurs on the dihydroflavonol. However, in our study overexpression of the whole flavonoid pathway in *N. benthamiana* in tandem with the CYP75A42 v.2 from Norway spruce resulted only in the detection of 2,3-(*trans*)-(+)-gallocatechin. No other 5'-hydroxylated flavonoids, including dihydromyricetin and leucodelphinidin could be detected in transformed *N. benthamiana* leaves. However, leucocyanidin was also not detected in our analyses, probably due to its lability (Fischer et al., 2003). Our data therefore indicates that 5' hydroxylation of 3,4-dihydroxylated flavonoids in Norway spruce occurs preferentially during the last step of the flavonoid biosynthetic pathway, producing 2,3-(*trans*)-(+)-gallocatechin from 2,3-(*trans*)-(+)-catechin. Several other lines of evidence support this result: Untargeted metabolite analysis of the Norway spruce genotype used in this study revealed the presence of the flavonols kaempferol and quercetin as well as the dihydroflavonol dihydroquercetin, but no trihydroxylated dihydroflavonols or flavonols were detected. Furthermore, in a previous study LAR enzymes from Norway spruce, catalyzing the last step in 2,3-(*trans*)-(+)-catechin biosynthesis, did not

accept the trihydroxylated substrate leucodelphinidin in *in vitro* enzyme assays (Hammerbacher et al., 2014).

2.4. Gallocatechin inhibits E. polonica *melanin biosynthesis more strongly than catechin, while catechin is a stronger inhibitor of growth*

To test the effects of 2,3-(*trans*)-(+)-gallocatechin on fungal growth, potato dextrose medium prepared with 1 mg mL^{-1} gallocatechin or catechin was inoculated with *E. polonica*. Fresh *E. polonica* mycelium is white, but turns black after a few days in culture with the formation of melanin. However, gallocatechin caused a striking delay in melanin formation (Figure 7 A). The rate of melanin appearance in cultures with gallocatechin was approximately 6 mm d^{-1}, significantly lower than in cultures with catechin (approximately 8 mm d^{-1}) ($p = 0.06$) or with no flavan-3-ol at all (approximately 10 mm d^{-1}) ($p < 0.005$). The effect of the flavan-3-ols on growth gave a different pattern of results. Here 2,3-(*trans*)-(+)-catechin slowed fungal growth significantly compared to the control ($p < 0.001$), more strongly than gallocatechin did (Figure 7 B). Our data thus suggests that gallocatechin and catechin both negatively impact on fungal growth and metabolism, but not in the same manner.

Fungal melanin is synthesized through either the dihydroxyphenylalanine or the dihydroxynaphthalene biosynthetic pathways (Langfelder et al., 2003). In both cases polymerization of monomeric precursor compounds is thought to occur via oxidative processes catalyzed by tyrosinases or laccases. Flavan-3-ols might inhibit melanin formation by serving as anti-oxidants since 3', 4', 5'-hydroxylated flavonoids are much stronger anti-oxidants under acidic conditions than their 3', 4' counterparts (Lee et al., 2014). 2,3-(*trans*)-(+)-Gallocatechin may therefore be an especially strong inhibitor of fungal melanin polymerization by scavenging radicals (Katiyar et al., 1994). Recent studies on human melanin biosynthesis have shown the same trend with gallocatechin and epigallocatechin-gallate inhibiting tyrosinase activity more than catechin and epicatechin and thereby significantly decreasing the formation of the dark-pigmented polymeric product (Peter et al., 2017).

The greater growth inhibition of catechin compared to gallocatechin is more difficult to explain as both compounds have been shown to have similar activities in human medicine. Both compounds also inhibit fungal proliferation. In *in vitro* assays catechin was shown to inhibit the mycelial growth of *H. annosum* (Nemesio-Gorriz et al., 2016) and the coffee rust *Hemileia*

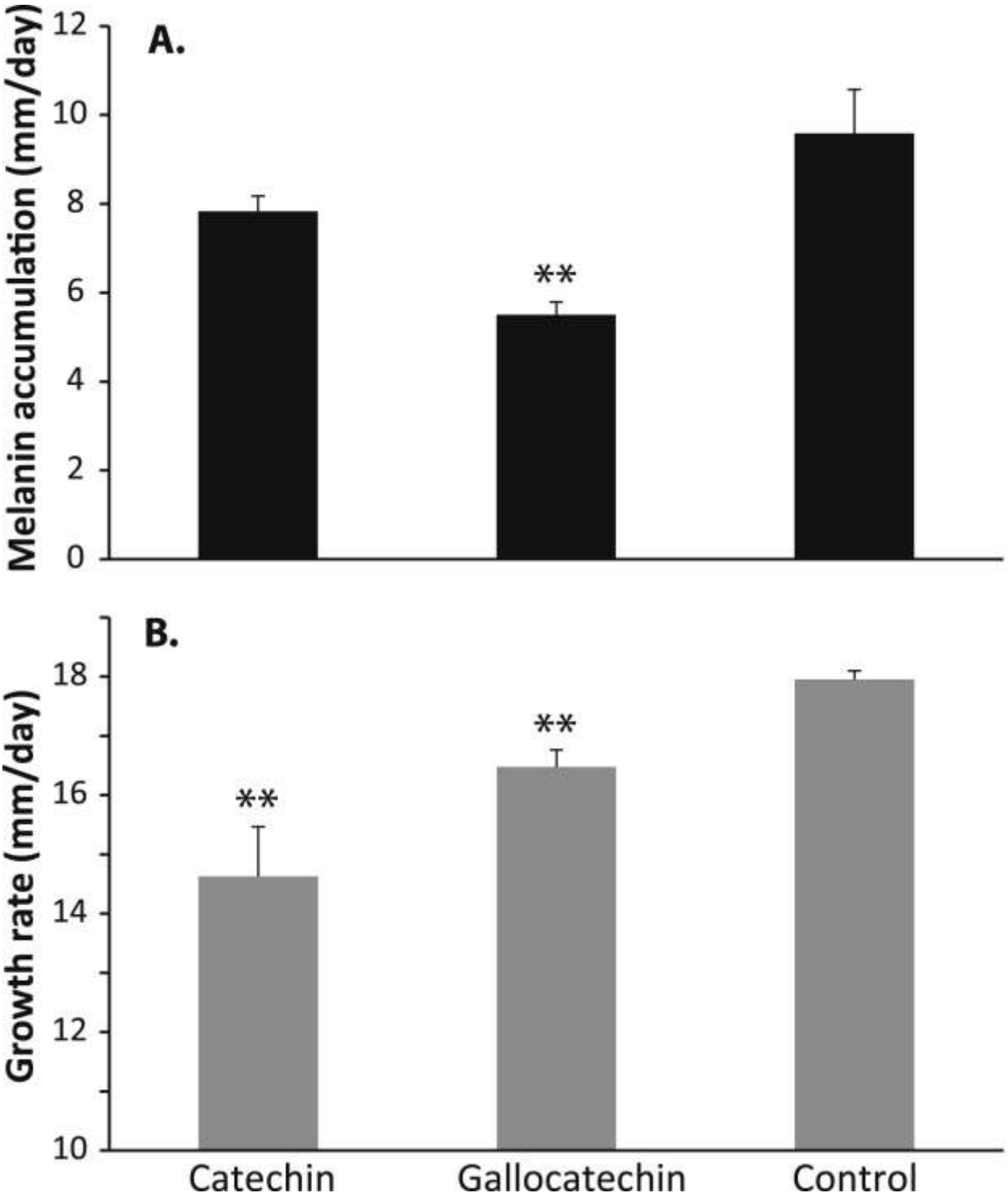

Figure 7: Catechin and gallocatechin have different effects on fungal growth and melanin pigment production. The figure depicts accumulation of melanin (A) and growth (B) of *E. polonica* cultures per day on artificial medium containing 1 mg mL^{-1} of either of the flavan-3-ols, catechin (dihydroxylated B ring) or gallocatechin (trihydroxylated B ring) ($p = 0.005$; $n = 4$; error bars = SE; stars denote treatments significantly different from the control).

vastatrix (de Colmenares et al., 1998). In plants, transgenic *Populus tomentosa* overexpressing LAR to produce more catechin was more resistant to infection by *Marssonina brunnea* than the untransformed wild-type (Yuan et al., 2012), while *Populus nigra* genotypes with higher levels of catechin were more resistant to infection by *Melampsora larici-populina* (Ullah et al., 2017). Exogenous application of epicatechin to plants was shown to inhibit fungal infection, as less infection occurred on coffee inoculated with *Colletotrichum kahawae* spores that had been suspended in 4 mM epicatechin compared to a control where spores had been suspended in water (Chen et al., 2006). The broad specificity of catechin and epicatechin in the inhibition of growth of fungi from different phylogenetic linages indicates that these compounds may interfere with conserved metabolic processes involved in fungal growth, but further studies are required to elucidate their precise mechanism of action.

3. Experimental

3.1. Fungal inoculation of Norway spruce

Five-year old Norway spruce saplings from the clone S21K0420117, originating from a Skogforsk (Sweden) tree improvement program, were grown in 5 L pots in an outdoor plot at the MPI-CE, Jena, Germany. Saplings were grown in a mixture of peat:sand (1:1, v:v) and watered regularly. The blue stain fungus, *E. polonica* isolate K2014 (*Kandassamy*, isol. Ex. bark beetle gallery, Thuringian Forest, Gotha, Germany), was grown on potato dextrose agar (Difco, BD, New Jersey, USA) at 25 ºC for 7 d in the dark. Saplings were inoculated with this culture in June 2014. A 5 mm cork borer was used to remove a circular piece of bark from the lower stems of the saplings. A similar-sized disk of the fungal culture was inserted into the wound and sealed with Parafilm. Sterile agar disks were used in control treatments. Wood and bark from 2.5 cm above and below the point of inoculation (including the point of inoculation) was harvested from the saplings 2 and 7 d after inoculation and from all wounded control treatments which were inoculated with sterile agar. Bark and wood were separated and the sections above and below the inoculation point were pooled. At 14 and 28 d after inoculation, the fungus-infected lesions were separated into two areas comprising (1) 2.5 cm above and below the point of inoculation (inner lesion) and (2) sections from 2.5 cm to 4 cm above and below the point of inoculation (outer lesion). Bark and wood were separated and sections with equivalent distances above and below the inoculation point were pooled. Each treatment and each time point was replicated five times

(n = 5). Samples were flash frozen in liquid nitrogen after harvest and ground to a fine powder using a mortar and pestle.

3.2. Metabolite analysis

Finely ground plant tissue was lyophilized at 0.34 mbar pressure using an Alpha 1-4 LD plus freeze dryer (Martin Christ GmbH, Osterode, Germany). Approximately 20 mg of dried spruce tissue powder or 100 mg ground *N. benthamiana* leaf tissue was extracted twice for 4 h with 600 µL analytical grade methanol containing 10 µg mL^{-1} internal standard, apigenin-7-glucoside (Carl Roth GmbH, Karlsruhe, Germany). Monomeric flavan-3-ols were analyzed by LC-tandem mass spectrometry on an Agilent 1200 HPLC system (Agilent, Santa Clara, CA, United States) coupled to an API 3200 mass analyzer (Sciex, Darmstadt, Germany) using the protocols described in Hammerbacher et al. (2014). Hydrolysis of polymeric PAs and subsequent analysis was also performed following published protocols (Hammerbacher et al., 2014).

3.3. Identification of F3'5'H candidate sequences and phylogenetic analysis

Warren et al. (2015) identified 2 *F3'5'H* candidate genes in the *P. glauca* genome (CYP 75A14 v. 2 and CYP75A63). These sequences were downloaded from NCBI and used in BLASTN searches against all *Picea* transcript assemblies in the conifer genome database (http://congenie.org/blast). Transcripts with high identity to CYP75A14 from *P. abies, P. glauca* and *P. sitchensis* were assembled into full-length contigs using DNA-STAR (Lasergene Genomics Suite, Madison, WI, USA). Gateway-compatible primers were designed for the 5' and 3' ends of the full length transcript of *P. abies* which was then amplified from cDNA using Phusion Taq (New England Biolabs, Ipswich, MA, USA) and cloned into pDONR 207 (Invitrogen, Carlsbad, CA, USA) using BP clonase II (Invitrogen). The cloned PCR product was sequenced with pDONR F and R primers using standard Sanger sequencing protocols. As BLAST searches did not yield any transcript sequences for CYP75A63, primers were designed using the transcript predicted by Warren et al. (2015). Amplification of this gene, however, did not succeed, despite using multiple cDNA samples derived from various *P. abies* and *P. glauca* clones and tissue-types. As this gene was not expressed in our Norway spruce genotype, it was excluded from further studies.

Protein sequences for characterized F3’5’H enzymes from different plant species were downloaded from NCBI and aligned with the translated nucleotide sequences of CYP 75A14 v. 2 from *P. abies*, *P. glauca* and *P. taeda* using the MAFFT web interface (http://mafft.cbrc.jp/alignment/server/) and imported into MEGA v.6 (Kumar et al., 2016; Center for Evolutionary Medicine and Informatics, Tempe, AZ, USA). The evolutionary history of F3’5’H enzymes was inferred by using the Maximum Likelihood method based on the Jones et al. (1992) model. The tree with the highest log likelihood (-8410.1395) is shown. The percentage of trees in which the associated taxa cluster together is shown next to the branches. Bootstrap values below 70 are not shown. Initial tree(s) for the heuristic search were obtained automatically by applying Neighbor-Join and BioNJ algorithms to a matrix of pairwise distances estimated using a JTT model, and then selecting the topology with superior log likelihood value. A discrete Gamma distribution was used to model evolutionary rate differences among sites (5 categories (+*G*, parameter = 0.4822)). The tree is drawn to scale, with branch lengths measured as the number of substitutions per site. The analysis involved 23 amino acid sequences. All positions with less than 95% site coverage were eliminated. That is, fewer than 5% alignment gaps, missing data, and ambiguous bases were allowed at any position. There were a total of 498 positions in the final dataset.

3.4. Heterologous expression of PaF3’5’H in N. benthamiana

The entire pathway for flavan-3-ol formation was heterologously expressed in *N. benthamiana* in order to characterize the function of the *PaF3’5’H* identified in this study. *PaCHS3* (Hammerbacher et al., 2011), *PaF3H1* (characterized in this study), *PaF3’H1* (characterized in this study), *MdDFR* (Fischer et al., 2003) and *PaLAR3* (Hammerbacher et al., 2014) were amplified and cloned into pDONR 207 as described in section 3.3. After sequence verification, these constructs were each subcloned into the pEAQ-HT-DEST1 vector (Sainsbury et al., 2012) using LR clonase. Plasmids with inserts were individually transformed into the *A. tumefaciens* strain GV3101. The bacteria were prepared for transformation following the protocols of Sainsbury et al. (2012). For *N. benthamiana* transformation, the following combinations were mixed together: *CHS, F3H* and *F3’5’H* (negative control), *CHS, F3H* and *F3’H* with or without *F3’5’H; CHS, F3H, DFR* and *F3’H* with or without *F3’5’H*; or *CHS, F3H, DFR, LAR* and *F3’H* with or without *F3’5’H*. Six week old *N. benthamiana* plants grown under

a 14 h light/10 h dark cycle at 25 ºC and 50 % relative humidity were transformed by vacuum infiltration (5 replicate plants per treatment combination).

N. benthamiana was transformed by immersing the leaves in the solution containing bacterial mixtures in an airtight chamber. Vacuum was applied to the chamber until the air pressure reached 50 mbar. Subsequently the vacuum was suddenly released from the chamber to ensure rapid infiltration of the bacteria into the stomata. Plants were grown for 7 d in the same conditions as described above before leaves were harvested, lyophilized and approximately 100 mg tissue extracted with absolute methanol for analysis.

3.5. Quantitative RT PCR

RNA was extracted from spruce bark and wood as described in Hammerbacher et al. (2014) using the Stratec Plant RNA mini kit (Stratec, Birkenfeld, Germany). RNA was reverse-transcribed to cDNA using Superscript v. II (Invitrogen). Approximately 100 ng cDNA was used per PCR reaction. qRT-PCR was performed with the Kappa SYBR Fast qPCR kit (Kappa Biosystems, Boston, MA, USA) and a CFX96 – Real-Time System (Bio-Rad, Hercules, CA, USA) following the manufacturer's specifications. *PaF3'5'H* was amplified using PaF3'5'H-F (GACATGGTCTGGGCAG) and PaF3'5'H-R (GTTTGAGAATATTCTGGAGCATG). The PCR was normalized using *PaUBI* (Schmidt et al., 2010; GB:EF681766.1) and calibrated to the 2 d wound-treatment. The means of 3 technical replicates from 5 biological replicates per treatment group were used to calculate the relative transcript abundance according to Pfaffl et al. (2001).

3.6. Fungal growth and melanin accumulation on 2,3-(*trans*)-(+)-*catechin and* 2,3-(*trans*)-(+)-*gallocatechin*

Growth of *E. polonica* on potato dextrose medium containing 0.5 mg mL^{-1} 2,3-(*trans*)-(+)-catechin or 2,3-(*trans*)-(+)-gallocatechin was determined in Petri dishes using the protocols described by Hammerbacher et al. (2014). In brief, the compounds were added to the medium in DMSO (20 mg mL^{-1}) just before the medium was dispersed into Petri dishes. Fungal growth of five replicates per compound was measured daily until the fungus grew to the edges of the Petri dish. The appearance of black-colored mycelium from the point of inoculation was also recorded on a daily basis. The progression of melanin appearance as well as fungal growth was plotted for

each Petri dish and a linear curve was fitted. The growth rate as well as the rate of melanin appearance was determined by the gradient of the fitted curve.

3.7. Statistical analysis

All data were subjected to a Shapiro-Wilk test for normality and non-normal data were transformed with the log or (1+log) function. Transformed or non-transformed data were analyzed using two- or one-way ANOVAs. Following this, Tukey's post-hoc test was used on data showing significant differences using a 5% confidence interval.

ACKNOWLEDGEMENTS

We would like to thank the Max Planck Society for financial support and the horticulturalists of the MPI-CE for assistance in maintaining the plant material.

References

Castellarin, S. D., Di Gaspero, G., Marconi, R., Nonis, A., Peterlunger, E., Paillard, S., Adam-Blondon, A. F., Testolin, R., 2006. Colour variation in red grapevines (*Vitis vinifera* L.): genomic organisation, expression of flavonoid 3'-hydroxylase, flavonoid 3', 5'-hydroxylase genes and related metabolite profiling of red cyanidin-/blue delphinidin-based anthocyanins in berry skin. BMC Genomics 7, 12.

Chen, Z. J., Liang, J. S., Zhang, C. H., Rodrigues, C. J., 2006. Epicatechin and catechin may prevent coffee berry disease by inhibition of appressorial melanization of *Colletotrichum kahawae*. Biotechnol. Lett. 28, 1637-1640.

Danielsson, M., Lundén, K., Elfstrand, M., Hu, J., Zhao, T., Arnerup, J., Ihrmark, K., Swedjemark, G., Borg-Karlson, A.-K., Stenlid, J., 2011. Chemical and transcriptional responses of Norway spruce genotypes with different susceptibility to *Heterobasidion* spp. infection. BMC Plant Biol. 11, 154.

de Colmenares, N. G., Ramírez-Martínez, J. R., Aldana, J. O., Ramos-Niño, M. E., Clifford, M. N., Pékerar, S., Méndez, B., 1998. Isolation, characterisation and determination of biological activity of coffee proanthocyanidins. J. Sci. Food and Agric. 77, 368-372.

Dixon, R. A., Xie, D. Y., Sharma, S. B., 2005. Proanthocyanidins - a final frontier in flavonoid research? New Phytol. 165, 9-28.

Fischer, T. C., Halbwirth, H., Meisel, B., Stich, K., Forkmann, G., 2003. Molecular cloning, substrate specificity of the functionally expressed dihydroflavonol 4-reductases from *Malus domestica* and *Pyrus communis* cultivars and the consequences for flavonoid metabolism. Arch. Biochem. Biophys. 412, 223-230.

Franceschi, V. R., Krokene, P., Christiansen, E., Krekling, T., 2005. Anatomical and chemical defenses of conifer bark against bark beetles and other pests. New Phytol. 167, 353-375.

Hammerbacher, A., Paetz, C., Wright, L. P., Fischer, T. C., Bohlmann, J., Davis, A. J., Fenning,

T. M., Gershenzon, J., Schmidt, A., 2014. Flavan-3-ols in Norway spruce: biosynthesis, accumulation, and function in response to attack by the bark beetle-associated fungus *Ceratocystis polonica*. Plant Physiol. 164, 2107-2122.

Hammerbacher, A., Ralph, S. G., Bohlmann, J., Fenning, T. M., Gershenzon, J., Schmidt, A., 2011. Biosynthesis of the major tetrahydroxystilbenes in spruce, astringin and isorhapontin, proceeds via resveratrol and is enhanced by fungal infection. Plant Physiol. 157, 876-890.

Hammerbacher, A., Schmidt, A., Wadke, N., Wright, L. P., Schneider, B., Bohlmann, J., Brand, W. A., Fenning, T. M., Gershenzon, J., Paetz, C., 2013. A common fungal associate of the spruce bark beetle metabolizes the stilbene defenses of Norway spruce. Plant Physiol. 162, 1324-1336.

Holton, T. A., Brugliera, F., Lester, D. R., Tanaka, Y., Hyland, C. D., Menting, J., Lu, C.-Y., Farcy, E., Stevenson, T. W., Cornish, E. C., 1993. Cloning and expression of cytochrome P450 genes controlling flower colour. Nature 366, 276.

Ishiguro, K., Taniguchi, M., Tanaka, Y., 2012. Functional analysis of *Antirrhinum kelloggii* flavonoid 3′-hydroxylase and flavonoid 3′, 5′-hydroxylase genes; critical role in flower color and evolution in the genus *Antirrhinum*. J. Plant Res. 125, 451-456.

Jones, D. T., Taylor, W. R., Thornton, J. M., 1992. The rapid generation of mutation data matrices from protein sequences. Computer applications in the biosciences: CABIOS 8, 275-282.

Katiyar, S. K., Agarwal, R., Mukhtar, H., 1994. Inhibition of spontaneous and photo-enhanced lipid peroxidation in mouse epidermal microsomes by epicatechin derivatives from green tea. Cancer Lett. 79, 61-66.

Krokene, P., 2015. Conifer defense and resistance to bark beetles, in: Hofstetter, R. W. (Ed), Bark beetles: biology and ecology of native and invasive species. Elsevier Academic Press, pp. 177-207.

Krokene, P., Solheim, H., 1998. Assessing the virulence of four bark beetle-associated bluestain fungi using Norway spruce seedlings. Plant Path. 47, 537-540.

Kumar, S., Stecher, G., Tamura, K., 2016. MEGA7: Molecular Evolutionary Genetics Analysis version 7.0 for bigger datasets. Mol. Biol. Evol. 33, 1870-1874.

Langfelder, K., Streibel, M., Jahn, B., Haase, G., Brakhage, A. A., 2003. Biosynthesis of fungal melanins and their importance for human pathogenic fungi. Fungal Genet. Biol. 38, 143-158.

Lee, L.-S., Kim, S.-H., Kim, Y.-B., Kim, Y.-C., 2014. Quantitative analysis of major constituents in green tea with different plucking periods and their antioxidant activity. Molecules 19, 9173-9186.

Liu, C., Wang, X., Shulaev, V., Dixon, R. A., 2016. A role for leucoanthocyanidin reductase in the extension of proanthocyanidins. Nature Plants 2, 16182.

Nemesio-Gorriz, M., Hammerbacher, A., Ihrmark, K., Källman, T., Olson, Å., Lascoux, M., Stenlid, J., Gershenzon, J., Elfstrand, M., 2016. Different alleles of a gene encoding leucoanthocyanidin reductase (PaLAR3) influence resistance against the fungus *Heterobasidion parviporum* in *Picea abies*. Plant Physiol. 171, 2671-2681.

Nystedt, B., Street, N. R., Wetterbom, A., Zuccolo, A., Lin, Y. C., Scofield, D. G., Vezzi, F., Delhomme, N., Giacomello, S., Alexeyenko, A., Vicedomini, R., Sahlin, K., Sherwood, E., Elfstrand, M., Gramzow, L., Holmberg, K., Hallman, J., Keech, O., Klasson, L., Koriabine, M., Kucukoglu, M., Kaller, M., Luthman, J., Lysholm, F., Niittyla, T., Olson,

A., Rilakovic, N., Ritland, C., Rossello, J. A., Sena, J., Svensson, T., Talavera-Lopez, C., Theissen, G., Tuominen, H., Vanneste, K., Wu, Z. Q., Zhang, B., Zerbe, P., Arvestad, L., Bhalerao, R., Bohlmann, J., Bousquet, J., Gil, R. G., Hvidsten, T. R., de Jong, P., MacKay, J., Morgante, M., Ritland, K., Sundberg, B., Thompson, S. L., Van de Peer, Y., Andersson, B., Nilsson, O., Ingvarsson, P. K., Lundeberg, J., Jansson, S., 2013. The Norway spruce genome sequence and conifer genome evolution. Nature 497, 579-584.

Paine, T., Raffa, K., Harrington, T., 1997. Interactions among scolytid bark beetles, their associated fungi, and live host conifers. Annu. Rev. Entomol. 42, 179-206.

Peter, B., Bosze, S., Horvath, R., 2017. Biophysical characteristics of proteins and living cells exposed to the green tea polyphenol epigallocatechin-3-gallate (EGCg): review of recent advances from molecular mechanisms to nanomedicine and clinical trials. Eur. Biophys. J. 46, 1-24.

Pfaffl, M. W., 2001. A new mathematical model for relative quantification in real-time RT–PCR. Nucleic Acids Res. 29, e45.

Punyasiri, P., Abeysinghe, I., Kumar, V., Treutter, D., Duy, D., Gosch, C., Martens, S., Forkmann, G., Fischer, T., 2004. Flavonoid biosynthesis in the tea plant *Camellia sinensis*: properties of enzymes of the prominent epicatechin and catechin pathways. Arch. Biochem. Biophys. 431, 22-30.

Sainsbury, F., Saxena, P., Geisler, K., Osbourn, A., Lomonossoff, G. P., 2012. Using a virus-derived system to manipulate plant natural product biosynthetic pathways. Methods Enzymol. 517, 185-202.

Schlyter, P., Stjernquist, I., Bärring, L., Jönsson, A. M., Nilsson, C., 2006. Assessment of the impacts of climate change and weather extremes on boreal forests in northern Europe, focusing on Norway spruce. Clim. Res. 31, 75-84.

Schmidt, A., Waechtler, B., Temp, U., Krekling, T., Seguin, A., Gershenzon, J., 2010. A bifunctional geranyl and geranylgeranyl diphosphate synthase is involved in terpene oleoresin formation in *Picea abies*. Plant Physiol. 152, 639-655.

Seitz, C., Ameres, S., Schlangen, K., Forkmann, G., Halbwirth, H., 2015. Multiple evolution of flavonoid 3′, 5′-hydroxylase. Planta 242, 561-573.

Stadelmann, G., Bugmann, H., Wermelinger, B., Meier, F., Bigler, C., 2013. A predictive framework to assess spatio-temporal variability of infestations by the European spruce bark beetle. Ecography 36, 1208-1217.

Tanaka, Y., Brugliera, F., 2013. Flower colour and cytochromes P450. Phil. Trans. R. Soc. B 368, 20120432.

Tanner, G. J., Francki, K. T., Abrahams, S., Watson, J. M., Larkin, P. J., Ashton, A. R., 2003. Proanthocyanidin biosynthesis in plants - Purification of legume leucoanthocyanidin reductase and molecular cloning of its cDNA. J. Biol. Chem. 278, 31647-31656.

Ullah, C., Unsicker, S.B., Fellenberg, C., Constabel, C.P., Schmidt, A., Gershenzon, J., Hammerbacher, A., 2017. Flavan-3-ols are an effective chemical defense against rust infection. Plant Physiol. 175, 1560-1578.

Wadke, N., Kandasamy, D., Vogel, H., Lah, L., Wingfield, B. D., Paetz, C., Wright, L. P., Gershenzon, J., Hammerbacher, A., 2016. The bark-beetle-associated fungus, *Endoconidiophora polonica*, utilizes the phenolic defense compounds of its host as a carbon source. Plant Physiol. 171, 914-931.

Warren, R. L., Keeling, C. I., Yuen, M. M. S., Raymond, A., Taylor, G. A., Vandervalk, B. P., Mohamadi, H., Paulino, D., Chiu, R., Jackman, S. D., 2015. Improved white spruce

(*Picea glauca*) genome assemblies and annotation of large gene families of conifer terpenoid and phenolic defense metabolism. Plant J. 83, 189-212.
Xie, D. Y., Sharma, S. B., Dixon, R. A., 2004. Anthocyanidin reductases from *Medicago truncatula* and *Arabidopsis thaliana*. Arch. Biochem. Biophys. 422, 91-102.
Yuan, L., Wang, L., Han, Z., Jiang, Y., Zhao, L., Liu, H., Yang, L., Luo, K., 2012. Molecular cloning and characterization of PtrLAR3, a gene encoding leucoanthocyanidin reductase from *Populus trichocarpa*, and its constitutive expression enhances fungal resistance in transgenic plants. J. Exp. Bot. 63, 2513-2524.